JVST A
Journal of Vacuum Science & Technology A

Influence of quantum-confined device fabrication on semiconductor-laser theory

Cite as: J. Vac. Sci. Technol. A **39**, 032408 (2021); https://doi.org/10.1116/6.0000767
Submitted: 09 November 2020 . Accepted: 25 February 2021 . Published Online: 19 March 2021

Weng W. Chow, and Frank Jahnke

JVST A
Journal of Vacuum Science & Technology A

ARTICLE

avs.scitation.org/journal/jva

Influence of quantum-confined device fabrication on semiconductor-laser theory

Cite as: J. Vac. Sci. Technol. A **39**, 032408 (2021); doi: 10.1116/6.0000767
Submitted: 9 November 2020 · Accepted: 25 February 2021 ·
Published Online: 19 March 2021

Weng W. Chow[1,a)] and Frank Jahnke[2]

AFFILIATIONS

[1]Sandia National Laboratories, Albuquerque, New Mexico 87185-1086
[2]Institute for Theoretical Physics, University of Bremen, P.O. Box 330 440, 28334 Bremen, Germany

Note: This paper is part of the Special Topic Collection: Honoring Dr. Art Gossard's 85th Birthday and his Leadership in the Science and Technology of Molecular Beam Epitaxy.
[a)]**Electronic mail:** wwchow@sandia.gov

ABSTRACT

Among Professor Arthur Gossard's many contributions to crystal growth are those resulting in important improvements in the quality and performance of quantum-well and quantum-dot semiconductor lasers. In celebration of his 85th birthday, we review the development of a semiconductor laser theory that is motivated and guided, in part, by those advances. This theory combines condensed matter theory and laser physics to provide understanding at a microscopic level, i.e., in terms of electrons and holes, and their interaction with the radiation field while influenced by the lattice.

I. INTRODUCTION

This paper traces the evolution of a laser theory undergoing development, with the goal of sufficient predictive capability to describe, based on the epitaxial growth sheet, gain medium performance and laser device behavior. The starting points are that carriers (1) obey Fermi-Dirac statistics, (2) as charged particles they interact strongly among themselves and with the lattice, and (3) with an electromagnetic field via a polarization from electron-hole pairs. The progress draws upon laser physics,[1] many-body semiconductor theory,[2] and equally importantly, motivation and guidance from successes in device fabrication.[3–6]

II. EARLY DAYS

Even today, calculations of semiconductor laser properties often assume free (noninteracting) carriers.[7,8] While these calculations provide some useful insight, e.g., into band structure influence, inadequacies appear with high-quality samples and advanced laser structures. There, one sees signatures of subtle many-body Coulomb effects.[9]

An early indication is the threshold behavior of vertical-cavity surface-emitting lasers (VCSELs).[10] The high finesse optical resonator, functioning as a sensitive spectrometer, translates changes in the overlap between resonator resonance and gain spectrum into measurable changes in lasing threshold current. The observed VCSEL temperature sensitivity (dots in Fig. 1) was thought to be from the temperature dependence of the cavity-gain overlap. This turned out to be only partly true. The dashed curve in Fig. 1 is from free-carrier theory, taking into account the separate temperature dependences of cavity resonances and gain spectrum. An obvious discrepancy appears at temperatures below the threshold current minimum. The solid curve, from a many-body laser calculation, reproduces the more symmetrical temperature dependence observed in experiments. The better agreement comes from one of the many-body modifications to the excitation dependence of the gain spectrum, in this case, the bandgap renormalization.[11]

The implementation of carrier quantum confinement in devices[4] greatly influences the direction of semiconductor laser research. Soon after the observation of many-body effects in VCSELs, detailed measurements of gain spectra from high-quality quantum-well active regions[13] came up with a difficult challenge for the theorists. The measurements revealed shortcomings with the then many-body calculation, which stopped at the Hartree–Fock level. Figure 2(a) shows the significant errors in reproducing the spectral shape and carrier density dependence, regardless of the choice of carrier densities and the dephasing rate.

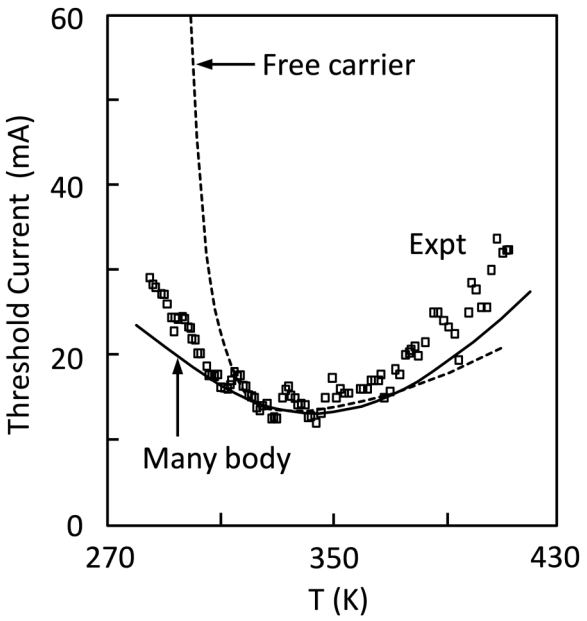

FIG. 1. Lasing threshold current vs temperature for a VCSEL. The dots are from the experiment, the dashed and solid curves are from calculations using a free-carrier and a many-body laser theory, respectively. Both calculations accounted for band structure details, such as the valence band mixing due to quantum confinement and strain. The difference is that the free-carrier calculation assumed Coulomb interaction among carriers to be negligible because of plasma screening, while the many-body calculations treated the interaction at the Hartree–Fock (mean-field) level. While the laser, with a gain medium consisting of three 8 nm $In_{0.2}Ga_{0.8}As$ quantum wells between GaAs barriers, was MOVCD grown, MBE contributed importantly to the early vertical-cavity laser experiments as described in Refs. 3 and 12. Reprinted with permission from W. W. Chow, S. W. Corzine, and L. A. Coldren, App. Phys. Lett. **66**, 2460 (1995). Copyright 1995, AIP Publishing LLC.

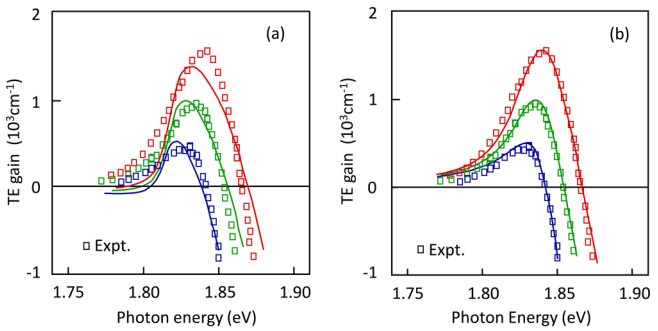

FIG. 2. (a) Gain spectra for a 6.8 nm $Ga_{0.41}In_{0.59}P/(Al_{0.5}Ga_{0.5})_{0.5}In_{0.49}P$ quantum well. The points are from the experiment at injection currents of 100, 140, and 180 mA. The curves are from calculations where many-body effects are at the Hartree–Fock level. The best fit to the experiment is from choosing a dephasing rate of $1/T_2 = 10^{13}$ s^{-1} and carrier densities of $N = 2.6 \times 10^{12}$, 3.0×10^{12}, 3.4×10^{12}cm^{-2}. (b) The curves are from extending the many-body theory to include scattering effects within the second Born and Markov approximations. The only input to the calculations is the band structure and the carrier densities, which were chosen to match the transparency energies of the measured spectra.

The solution was challenging because it required extending the many-body effects to the next Coulomb correlation stage, a step that was both derivation- and numerical-wise demanding.[14] Carrier collisions are responsible for these correlations giving rise to dephasing, population relaxation, and plasma screening. Once implemented, the improvement was immediate as depicted in Fig. 2(b).[15] The unphysical absorption below the bandgap was eliminated, and the shape and excitation dependences of the gain spectrum were described almost exactly. Most importantly, the improvement came with the removal of the dephasing rate ($1/T_2$) as a free parameter. This resulted in significantly more powerful predictive capability.

Physics wise, the newer gain theory uncovered a new and interesting aspect of the system-reservoir interaction. When the system is its own reservoir (as with carriers where the reservoir consists of other identical electrons or holes), the dephasing has both diagonal and nondiagonal contributions. As such, the answer to the longstanding question, "What is the semiconductor lineshape function?" is, "None, because strictly speaking, dephasing in semiconductors is not representable by an analytic function and definitely not by a Lorentzian function."

Another aspect of the many-body theory for the semiconductor gain medium is its capability to describe the nonequilibrium effects of excited carriers. At first, they became evident as an imbalance between the effective carrier temperature (assigned from the carriers mean kinetic energy) and the lattice temperature, as predicted by theory[16] and seen in experiments.[17] Another implication is kinetic hole burning, which—together with interaction-induced dephasing—are the main sources for gain nonlinearities. They lead to a reduction of the differential gain and thereby limit the small-signal modulation bandwidth of semiconductor lasers.[18]

Finally, the semiconductor laser theory provides an interface to material physics and carrier confinement engineering. The two physical effects here are changes in the single-particle energies of carriers in heterostructures and strain due to different lattice constants of adjacent materials. Both are directly used to control the carrier confinement in quantum-well and quantum-dot (QD) lasers. In terms of simulations, frequently, $\mathbf{k}\cdot\mathbf{p}$ models have been used to determine confinement energies, effective masses, and dipole- and Coulomb-interaction matrix elements. These are directly used in semiconductor Bloch equations for gain calculations, thereby providing an effective interface between material engineering and laser theory.

III. THE PRESENT

Similar to crystal growth, advances in the first-principles based laser theory take a while to come to fruition. In this section on the present status, we will discuss the results accumulated over several decades of theoretical developments. The impetus came from the crystal growth developments that enabled the progression of carrier confinement from quantum wells to quantum dots.[5] From the theory side, the transition from quasicontinuous to

discrete states requires revisiting gain behavior, where the manifestations of many-body interactions are noticeably different.[19]

Perhaps, the most challenging problem concerned carrier transport in quantum-dot lasers. The argument was the following. Based on carrier-phonon interaction matrix elements, the strongest contribution to carrier relaxation comes from longitudinal-optical (LO) phonons. However, the small energy dispersion of LO phonons means that the energy-conservation requirement from a second order perturbation treatment is likely not satisfied when the initial and final scattering states are separated by greater than an LO-phonon energy. While other relaxation channels exist, the energies involved are too small to be effective. Hence, the warning of a serious problem with quantum-dot devices: a phonon bottleneck.[20]

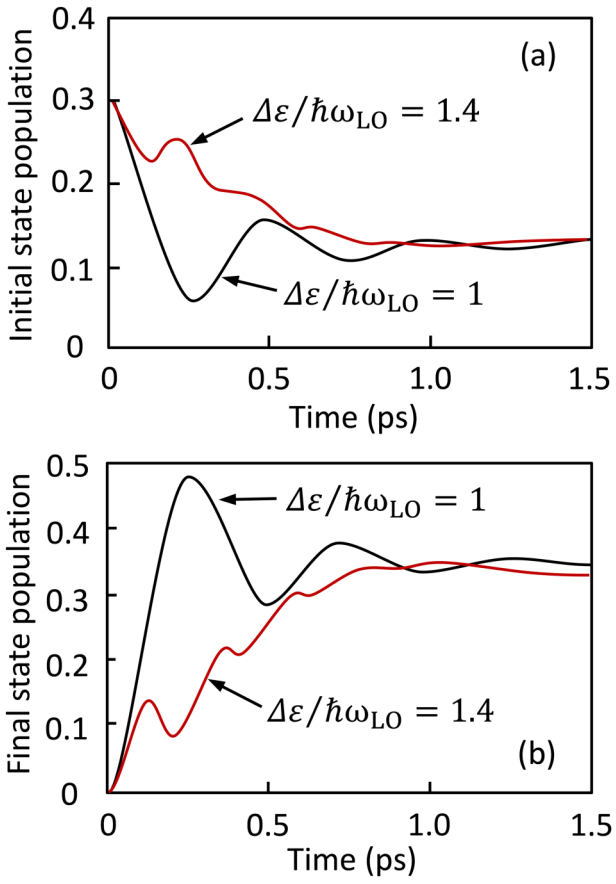

FIG. 3. Evolution of quantum-dot electron population from (a) initial p-shell to (b) final s-shell according to quantum kinetic calculations where electrons and LO phonons are treated as composite particles (polarons). As labeled, the curves are for initial state energy separation equal to the LO-phonon energy, and the initial state energy separation equals 1.4 times the LO-phonon energy. In the latter, the relaxation of electron population is finite, in contradiction to the prediction of a phonon bottleneck. Calculations are performed for $T = 300$ K. Adapted with permission from J. Seebeck, T. R. Nielsen, P. Gartner, and F. Jahnke, Phys. Rev. B **71**, 125327, (2005). Copyright 2005, American Physical Society.

However, quantum-dot lasers mostly perform without the phonon bottleneck problem. That led to many attempts to resolve the discrepancy. Some of the results led to a better understanding of quantum-dot physics. Examples include memory effects and the role of carriers in the quasicontinua in the wetting layer and embedding quantum well.[21,22] However, a direct answer remained elusive, until the realization that the perturbation/Markov approach is inadequate for describing quantum-dot scattering. Rather, one needs a nonperturbative treatment that considers a carrier and surrounding cloud of lattice distortions as a quasiparticle: a polaron.[23] With this quantum kinetic approach, the carrier-phonon scattering rate with initial and final scattering state separated by greater than the LO-phonon energy remains finite (Fig. 3).

Besides resolving the phonon bottleneck issue, laser gain theory with collisions treated at the level of quantum kinetic equations make possible the exact description of the intrinsic (homogeneously broadened) gain spectrum. The curve with the sharpest resonances in Fig. 4 shows, without ambiguity, the fundamental limit to gain and linewidth for InAs quantum dots embedded in an $In_{0.15}Ga_{0.85}As$ quantum well. To arrive at the homogeneously broadened spectrum with certainty is impossible with calculations requiring the dephasing rate ($1/T_2$) as an input parameter. With the homogeneously broadened spectrum, one can perform a statistical average over the spread of quantum-dot level energies, with standard deviation Δ_{inh} to obtain the inhomogeneously broadened

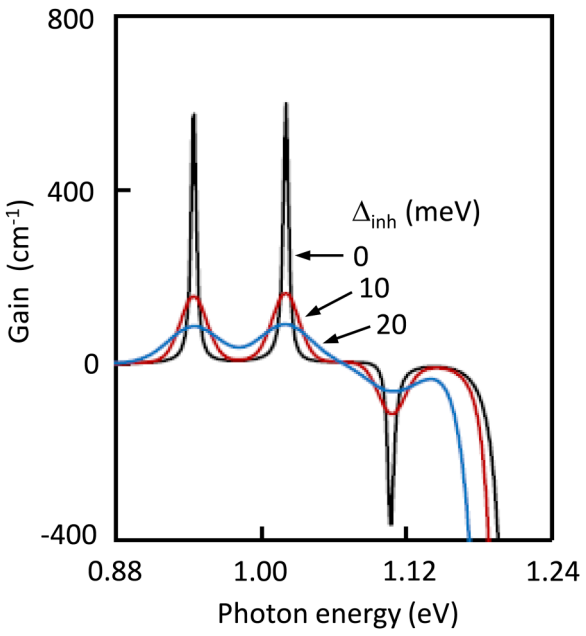

FIG. 4. Calculated gain spectra for the InAs/$In_{0.15}Ga_{0.85}As$ quantum-dot gain medium. The carrier and quantum-dot densities are 4×10^{11} cm^{-2} and 5×10^{10} cm^{-2}, respectively. The curve with the narrowest resonances is the homogeneously broadened spectrum. Its convolution with a distribution of transition energies with standard deviation Δ_{inh} gives the inhomogeneously broadened gain spectra (as labeled).

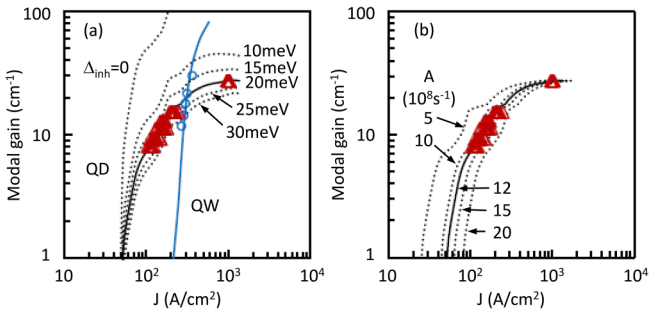

FIG. 5. Modal gain vs current densities for different (a) inhomogeneous broadening and (b) defect loss (Shockley–Read–Hall) coefficient. The curves are from calculations and the points are the measured threshold gain vs current density for lasers from the same wafer. Used together, the matching of theory and experiment helps monitor growth processes by providing a quantitative characterization of sample quality. Reprinted with permission from W. W. Chow, A. Y. Liu, A. C. Gossard, and J. E. Bowers, Appl. Phys. Lett. **107**, 171106, (2015). Copyright 2015, of AIP Publishing LLC.

gain spectra (Fig. 4). Matching features in spectra similar to these measured ones gives quantitative information (in the form of Δ_{inh}) that directly relates to the growth process. In contrast, the often-used spontaneous emission width contains contributions from both homogeneous broadening and quantum-dot variations. Section IV describes an approach to separate intrinsic and extrinsic contributions so that growth related imperfections might be isolated. We have been using it to systematically track quantum-dot uniformity in lasers from $\Delta_{inh} > 25$ meV, when it was first applied, to the recent values of $\Delta_{inh} = 10$ meV.[6]

IV. APPLICATIONS OF LASER THEORY

A. Determination of inhomogeneous broadening

Inhomogeneous broadening from quantum-dot dimension and composition variations remains a major obstacle to a quantum-dot laser realizing its full potential. In order to track progress made toward improving quantum-dot uniformity, it is important to have precise (quantitative) information on the inhomogeneous broadening in a sample.

Determining the inhomogeneous broadening through measurements alone is hindered by the difficulty in separating intrinsic and extrinsic effects. Working with experimentalists, we have developed an approach that takes advantage of a first-principles based quantum-dot gain theory (see Sec. III) to remove the intrinsic contributions so that inhomogeneous broadening can be quantified in terms of the standard deviation Δ_{inh} of the transition energies involved with ground state lasing.[24]

To apply the method, we fabricate from the wafer of interest, lasers with different cavity lengths (or equivalently, different threshold gains). Then, we use the lasers operating with threshold gains in the rollover region to determine Δ_{inh}. These are the lasers giving the experimental data points in Fig. 5(a) with threshold current densities >1 kA/cm^2. Central to the approach is recognizing that the quantum-dot peak gain saturates at a value depending on only the quantum-dot density and the inhomogeneous broadening. Therefore, regardless of the extrinsic effects, such as from defect carrier loss, all threshold gain versus current density curves for a given inhomogeneous broadening converge to a common maximum gain value after the onset of gain rollover [see Fig. 5(b)]. Also important for implementing the approach is a theory for calculating the homogeneously broadened (intrinsic) laser gain that is without free parameters (most importantly, without having a dephasing rate as an input parameter). Once Δ_{inh} is determined, the lower threshold lasers may be used to extract difficult to measure quantities, such as those listed in Table I from a study involving p-doping effects.[25]

TABLE I. Parameters extracted from theory/experiment comparison for InAs quantum-dot lasers on silicon with quantum-dot density 5×10^{10} cm^{-2} and different p-doping. SRH is an acronym for Shockley–Read–Hall.

Parameter	Sample A	Sample B	Sample C
p-dope density (cm^{-3})	UID	5×10^{17}	10^{18}
QD density (cm^{-2})	5×10^{10}	5×10^{10}	5×10^{10}
Inhomogeneous broadening Δ_{inh} (meV)	10	10	10
Defect (SRH) loss A (s^{-1})	1.29×10^{8}	1.31×10^{8}	2.63×10^{8}
Auger coefficient C (cm^6 s^{-1})	1.71×10^{-26}	1.71×10^{-26}	1.85×10^{-26}

B. Atomistic modeling of active materials

The source of inhomogeneous broadening is more directly accessible in atomistic models, which have been developed for quantum-dot active materials[26–28] and more recently for atomically thin semiconductors.[29] Individual quantum dots can be modeled on a three-dimensional lattice grid of atomic sites placed within a supercell. To describe, for example, InGaAs quantum dots, one can start from GaAs unit cells and replaces Ga by In atoms within the quantum dot, wetting layer, and barrier region according to the geometry and morphology of the structure. Alloys with a given In content or even concentration gradients across the quantum-dot or barrier regions can be simulated by randomly positioning only the desired percentage of In atoms. Of great help are high-resolution transmission electron microscopy investigations of the epitaxial grown structures, in which geometry, alloy concentration profiles, and strain distributions for individual quantum dots are analyzed. The simulation can directly rebuild such a particular quantum-dot structure with atomic resolution in a supercell containing millions of atoms. In general, various material systems like GaAs, GaN, and InP including quaternary alloys can be described.

The atomistic modeling is performed in several steps. First, a valence force field simulation is used to find new equilibrium positions of the individual atoms by minimizing the elastic energy. Then, a tight-binding Hamiltonian for the complete set of atoms is formulated. This leads to a huge but sparse tight-binding matrix, which can be diagonalized, thereby providing the band structure of the system. This includes the confinement energies of electrons and

holes in the nanostructure as well as their wave functions, which provide dipole and Coulomb-interaction matrix elements. The parameters of the tight-binding model (atomic on-site and hopping matrix elements) are chosen to reproduce *ab initio* results in bulk semiconductor calculations. The final step is to use the single-particle energies and interaction matrix elements in many-body absorption and gain calculations described above.

With present-day supercomputers, it is possible to repeat such a calculation for various individual quantum dots of different sizes, with variations of the alloy content, or studying experimentally observed concentration gradients. An example is given in Fig. 6. The individual contributions of each of these effects to the inhomogeneous broadening to absorption and gain spectra can thereby be disentangled.[28]

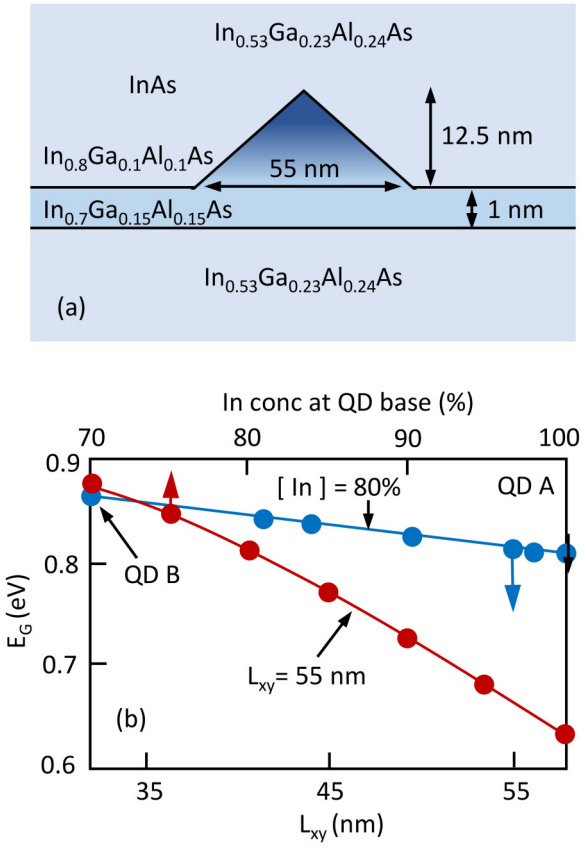

FIG. 6. (a) Cross section of the pyramidal quantum dot as determined from high-resolution scattering transmission electron microscopy with alloy concentrations extracted from the experiment. A supercell built out of elementary crystal unit cells has been constructed to match this geometry for an individual quantum dot. The alloyed structure is modeled by randomly placing In, Al, and Ga atoms at the cation positions according to the concentration profile. (b) Variation of the optical bandgap E_G for different members of the inhomogeneous quantum-dot ensemble. Each red and blue data point corresponds to a supercell simulation of a single quantum dot. Either the size (blue) or the In concentration (red) is varied in the range estimated from experimental data. QD A and QD B are members of the inhomogeneous ensemble on the same wafer with detailed experimental characterization. Reprinted with permission from E. Goldman, M. Paul, F. Krause, K. Muller, J. Kettler, T. Mehrtens, A. Rosenauer, M. Jetter, P. Michler, and F. Jahnke, Appl. Phys. Lett. **105**, 152102 (2014). Copyright 2014, AIP Publishing, LLC.

V. CONCLUSION

We conclude with a bird's eye view of the theory presently available for describing semiconductor lasers and emitters (Fig. 7). The philosophy is to start precisely with the physics entering into the theory. In this case, it is contained in a nonrelativistic Hamiltonian consisting of the energies from light-matter interaction and Coulomb interaction. There are two paths for proceeding. One leads to a theory for calculating gain and carrier-induced refractive index and their carrier density dependences, as induced by a laser field. The information is useful in two ways. It provides the gain parameters at saturated carrier density in the often-used class B semiconductor laser model.[30] It is also used in predicting general laser performance (such as light-current characteristics) when the saturated gain and carrier density are clamped at the threshold values.[18] The second path leads to a laser theory, where we invoke self-consistency by demanding the inducing laser field equals the field resulting from the induced gain and refractive index. The calculations give laser behavior for a given resonator configuration. A tradeoff is a less rigorous treatment of scattering effects than in the gain theory, which results in ambiguities arising from the choice of scattering rates. As shown in Fig. 7, these two branches evolved into several sub-branches, allowing for bandstructure engineering of active medium or numerical experiments on ideas for laser configurations. For more discussion, please refer to two reviews written especially for the nonspecialist.[19,31]

So, happy birthday, Professor Gossard. The samples produced by advances in crystal growth pioneered by you, your students, and colleagues help verify each stage of the theory development. They uncovered interesting physics, which led to novel devices that help justify the efforts of many physicists over a period of spanning decades. The theoretical efforts prove their worth by coming up with answers to questions such as "What is the lineshape function?" "Are semiconductor lasers homogeneously or inhomogeneously broadened?" "Why do quantum-dot devices not show a phonon bottleneck?" "Why is the dipole approximation valid for carriers which are delocalized?" "Are quantum-dot lasers better than quantum-well lasers?" Answering these questions would be difficult without input from carefully taken experimental data, such as the gain spectra provided to us by Professors Peter Blood and Peter Smowton from Cardiff University.

A particularly satisfying goal would be to see the theory routinely used in crystal growth and device fabrication. There has been some progress toward that direction. An example involves the design of VCSELs to operate optimally at desired temperatures. The incorporation of quantum kinetic theory into gain calculations, and the resulting elimination of scattering rates as free parameters, cannot be overemphasized. It helps device characterization, such as systematic and precise determination of quantum-dot inhomogeneous broadening and nonradiative loss rates.[24] It also provides expedient explorations of ideas for improving laser performance. Recent examples include the use of p-doping in quantum dots and the search to minimize linewidth enhancement effects to mitigate

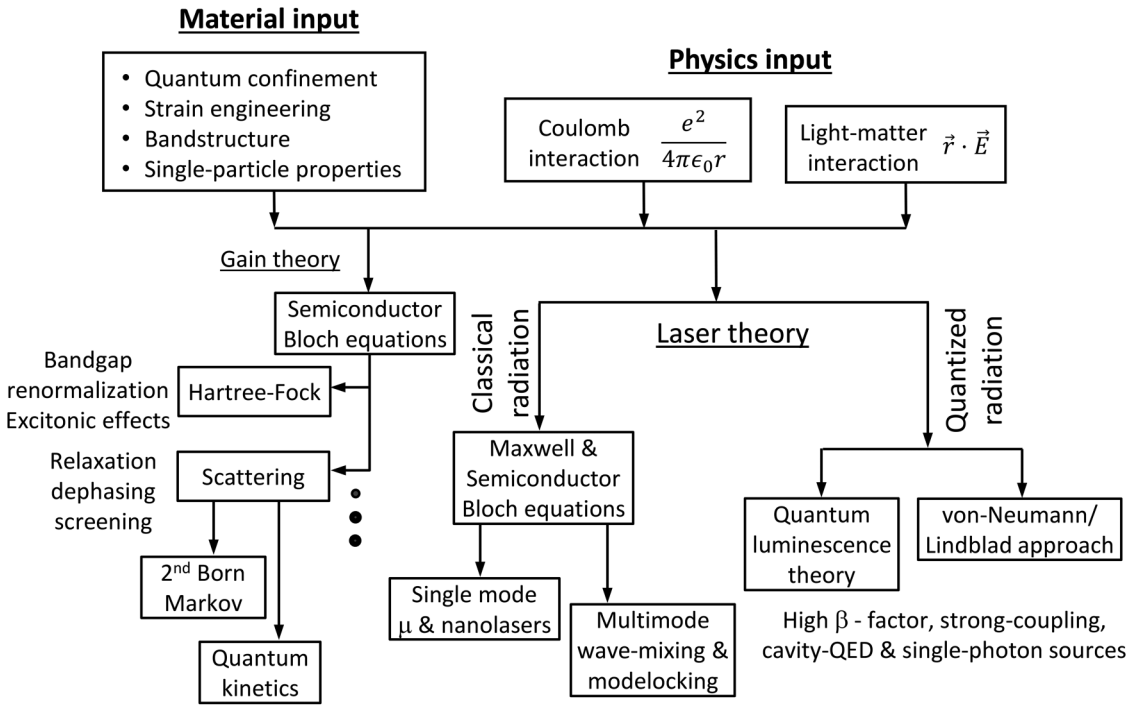

FIG. 7. Sketch showing the paths branching out from the general approach based on a many-body microscopic description of the gain medium. The difference between the gain theory and the laser theory involves balancing between rigor in treating scattering effects and maintaining reasonableness in numerical demand to facilitate parametric studies. With the gain theory, the optical response of a thin slice of the gain medium to an input laser field is calculated precisely (without free parameters) for a given carrier density. It is important to consider a gain slice sufficiently thin so that the linear response is valid. Doing so allows the scattering description by quantum kinetic equations. The laser theory accounts for saturation effects (thus eliminating the thin gain slice requirement) by simultaneously solving the coupled Maxwell and semiconductor-Bloch equations. Doing so is only numerically practical by approximating scattering effects with effective scattering rates that either is extracted from the experiment or from quantum kinetic calculations.

sensitivity to feedback and to maintain spectral stability during modulation or mode-lock operation.[25,32–34] In more top-level studies, the theory (because of its connection of microscopic physics and minimization of free parameters) helps guide the evaluation of new material systems and novel resonator concepts.[35] Further progress in the application of the theory to laser engineering depends importantly with collaborations with experimentalists. We gratefully acknowledge on-going collaborations with experimental groups of John Bowers (University of California, Santa Barbara), Frederic Grillot (Telecom Paris), Johann-Peter Reithmaier (Kassel University), and Gadi Eisenstein (Technion).

Lastly, we wish to note that many of the people contributing to the answers were at one time or the other at the Theory Semiconductor Physics Group of Professor Stephan Koch at the University of Marburg. The authors looked back fondly to those "Early Days" when the possibility of encountering serious difficulties was a sufficient reason to work on a problem.

ACKNOWLEDGMENTS

This work was supported in parts by the U.S. Department of Energy under Contract No. DE-NA0003525, the Deutsche Forschungsgemeinschaft, and the Center for Integrated Nanotechnologies (CINT) through a user proposal.

REFERENCES

[1]M. Sargent, III, M. O. Scully, and W. E. Lamb, Jr., *Laser Physics* (Addison-Wesley, Reading, 1974).
[2]H. Haug and S. W. Koch, *Quantum Theory of the Optical and Electronic Properties of Semiconductors* (World Scientific, Singapore, 1994).
[3]J. L. Jewell, H. M. Gibbs, A. C. Gossard, A. Passner, and W. Wiegmann, Mater. Lett. **1**, 148 (1983).
[4]A. C. Gossard, R. C. Miller, and W. Wiegmann, Surf. Sci. **174**, 131 (1986).
[5]R. Mirin, A. Gossard, and J. Bowers, Electron. Lett. **32**, 1732 (1996).
[6]J. C. Norman *et al.*, IEEE J. Quantum Electron. **55**(2), 2000511 (2019).
[7]G. H. B. Thompson, *Physics of Semiconductor Laser Devices* (Wiley, New York, 1980).
[8]S. L. Chuang, *Physics of Photonic Devices* (Wiley, New York, 1995).
[9]W. W. Chow and S. W. Koch, *Semiconductor-Laser Fundamentals: Physics of the Gain Materials* (Springer-Verlag, Berlin, 1998).
[10]D. B. Young, J. W. Scott, F. H. Peters, M. L. Majewski, B. J. Thibeault, S. W. Corzine, and L. A. Coldren, IEEE J. Quantum Electron. **29**, 2013 (1993).
[11]W. W. Chow, S. W. Corzine, and L. A. Coldren, Appl. Phys. Lett. **66**, 2460 (1995).

[12]J. L. Jewell, A. Scherer, S. L. McCall, A. C. Gossard, and J. H. English, Appl. Phys. Lett. **51**, 94 (1987).
[13]P. Blood, G. M. Lewis, P. M. Smowton, H. Summers, J. Thomson, and J. Lutti, IEEE J. Sel. Top. Quantum Electron. **9**, 1275 (2003).
[14]F. Jahnke *et al.*, Phys. Rev. Lett. **77**, 5257 (1996).
[15]W. W. Chow, P. M. Smowton, P. Blood, A. Girndt, and S. W. Koch, Appl. Phys. Lett. **71**, 157 (1997).
[16]F. Jahnke and S. W. Koch, Opt. Lett. **18**, 1438 (1993).
[17]U. Mohideen, R. E. Slusher, F. Jahnke, and S. W. Koch, Phys. Rev. Lett. **73**, 1785 (1994).
[18]L. A. Coldren, S. W. Corzine, and M. L. Masanovic, *Diode Lasers and Photonic Integrated Circuits*, 2nd ed. (John Wiley & Sons, Inc, New York, 2012).
[19]W. W. Chow and F. Jahnke, Prog. Quantum Electron. **37**, 109 (2013).
[20]H. Benisty, C. M. Sotomayor-Torres, and C. Weisbuch, Phys. Rev. B **44**, 10945 (1991).
[21]H. C. Schneider, W. W. Chow, and S. W. Koch, Phys. Rev. B **64**, 115315 (2001).
[22]H. C. Schneider, W. W. Chow, and S. W. Koch, Phys. Rev. B **70**, 235308 (2004).
[23]J. Seebeck, T. R. Nielsen, P. Gartner, and F. Jahnke, Phys. Rev. B **71**, 125327 (2005).
[24]W. W. Chow, A. Y. Liu, A. C. Gossard, and J. E. Bowers, Appl. Phys. Lett. **107**, 171106 (2015).
[25]Z. Zhang, D. Jung, J. C. Norman, P. Patel, W. W. Chow, and J. E. Bowers, Appl. Phys. Lett. **113**, 061105 (2018).
[26]E. Goldman *et al.*, Appl. Phys. Lett. **105**, 152102 (2014).
[27]E. Goldman, M. Lorke, T. Frauenheim, and F. Jahnke, Appl. Phys. Lett. **104**, 242108 (2014).
[28]C. Carmesin *et al.*, Phys. Rev. B **96**, 235309 (2017).
[29]A. Steinhoff, M. Rösner, F. Jahnke, T. O. Wehling, and C. Gies, Nano Lett. **14**, 3734 (2014).
[30]R. Lang and K. Kobayashi, IEEE J. Quantum Electron. **16**, 347 (1980).
[31]W. W. Chow and S. Reitzenstein, Appl. Phys. Rev. **5**, 041302 (2018).
[32]Z. Zhang, D. Jung, J. C. Norman, W. W. Chow, and J. E. Bowers, IEEE J. Sel. Top. Quantum Electron. **25**(6), 1900509 (2019).
[33]W. W. Chow, Z. Zhang, J. C. Norman, S. Liu, and J. E. Bowers, APL Photonics **5**, 026101 (2020).
[34]W. W. Chow, S. Liu, Z. Zhang, J. E. Bowers, and M. Sangent, III, Opt. Express **28**, 5317 (2020).
[35]W. W. Chow, M. Lorke, and F. Jahnke, IEEE J. Sel. Top. Quantum Electron. **17**, 1349 (2011).